Supplementary information

A universal method for planar lipid bilayer formation by freeze and thaw

Kaori Sugihara*, Bumjin Jang, Manuel Schneider, János Vörös and Tomaso Zambelli

Laboratory of Biosensors and Bioelectronics, Institute for Biomedical Engineering, ETH Zurich, Gloriastrasse 35, CH-8092 Zurich, Switzerland

* Corresponding author. e-mail: sugihara@biomed.ee.ethz.ch

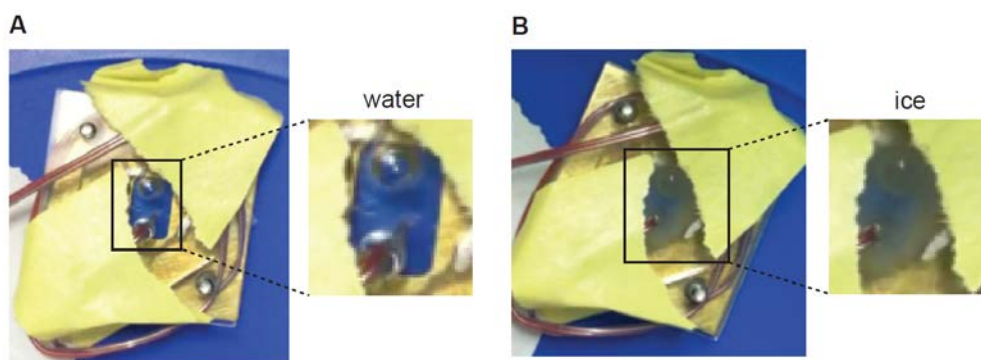**Images of the flowcell before and after the ice formation**

Figure S1 *Zoomed-in images of the flowcell (A) before and (B) after the ice formation*

In the text, we presented the temperature curve with a sudden jump that indicates super-cooling of the solution inside of the flowcell and the following nucleation for the ice formation. Figure S1 shows images of the flowcell (A) before and (B) after the sudden jump in temperature. The solution is transparent before the temperature jump, while it became semi transparent after the jump, proving that jump is associated with the ice formation.

Atomic force microscopy (AFM) and confocal laser scanning microscopy (CLSM) images of the assembled supported lipid bilayers (SLBs) <u>before the strong rinse</u>
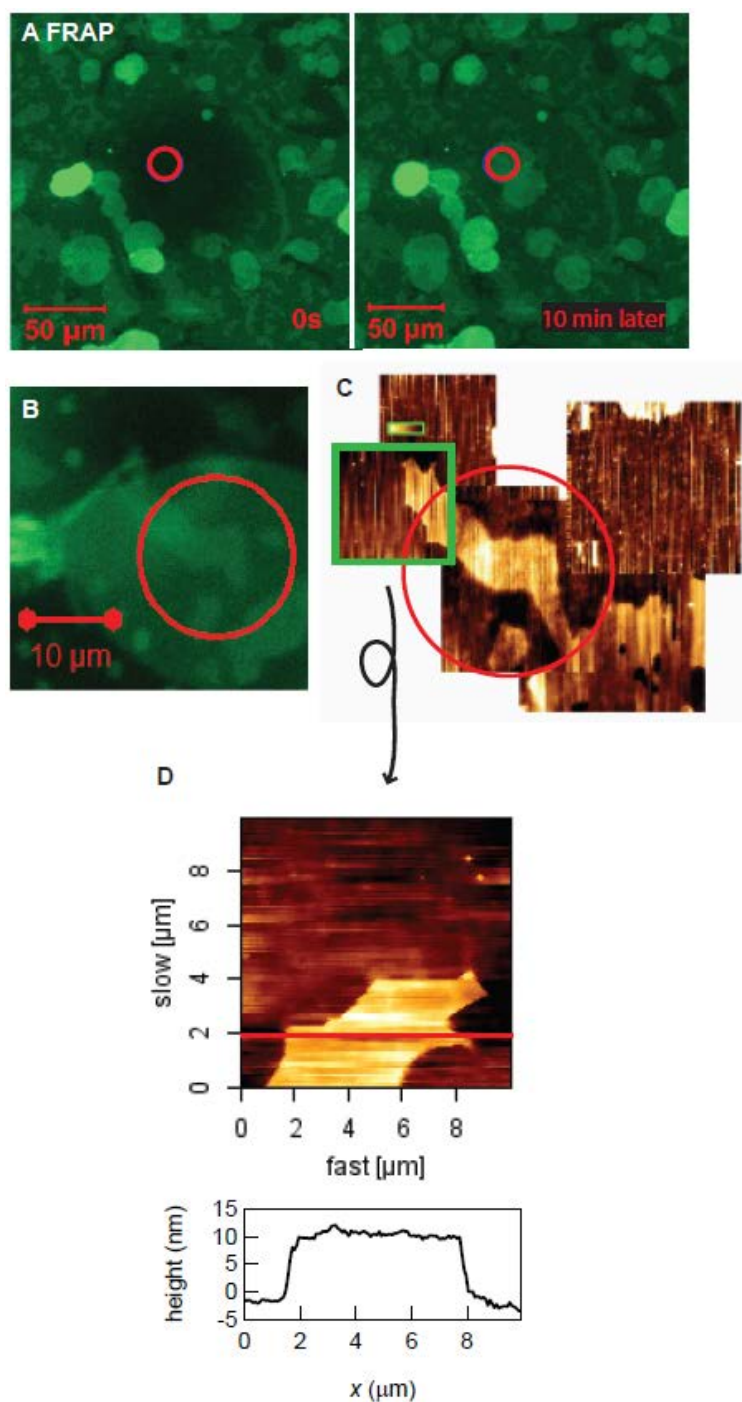

Figure S2 *Combined atomic force microscope (AFM) and confocal laser scanning microscope (CLSM) imaging of the SLBs formed by freeze and thaw (POPC + Nb_2O_5)*

(A) Fluorescence recovery after photobleaching (FRAP) indicates the fluidity of the formed lipid structures. **(B)** A zoomed-in CLSM image of the area around the red circle indicated in (A). **(C)** AFM images of the identical lipid object. The red circle corresponds to the red circle in the optical image (B). **(D)** the zoomed-in AFM image of the green square indicated in (C), and its cross section at the red line. Note that the image is rotated 90°clockwise.

As mentioned in the main text, although the surfaces after the freeze-thaw cycle show fluidity, their morphology is not homogenous. We characterized such surfaces by AFM (Figure S2). Note that the AFM images were obtained by tapping mode. Figure S2A shows fluorescence recovery after photobleaching (FRAP) images of a representative surface before the strong rinse. The good recovery indicates the fluidity of the lipid structure. We focused on the object indicated with the red circle in Figure S2A-C, and imaged it by CLSM (Figure S2B) and AFM (Figure S2C). The cross section of the zoomed-in AFM image of a part of the object (Figure S2D) shows that the height of the object is ~ 10 nm. Considering that we can remove such objects by the strong rinse, we assume they are multibilayers adsorbed on the lipid bilayer.

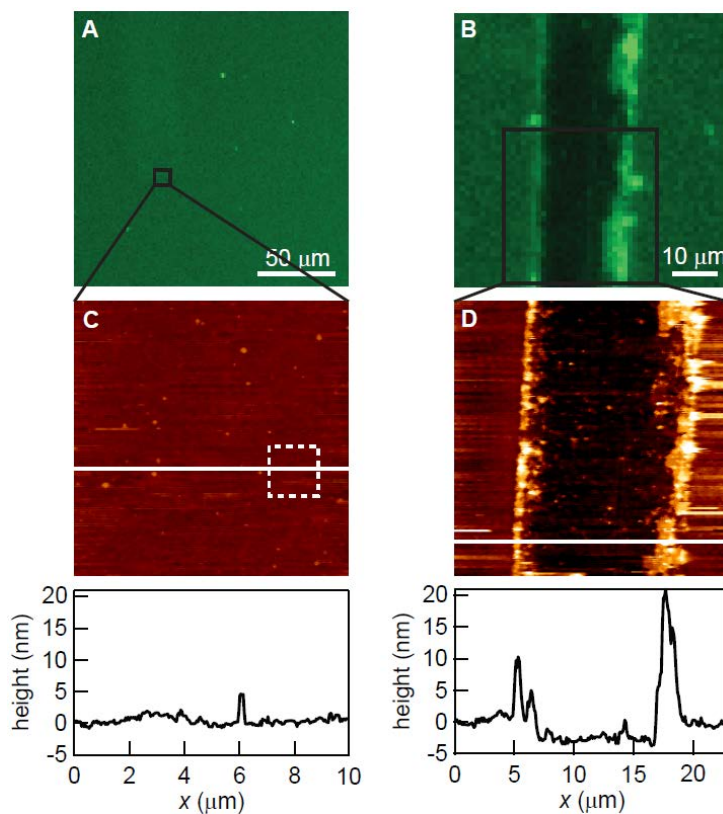**AFM and CLSM images of the assembled SLBs <u>after the strong rinse</u>**

Figure S3 *AFM and CLSM images of the SLB surfaces after the strong rinse*

The sample was fabricated as written in the main text with TiO_2 and 1,2-dielaidoyl-sn-glycero-3-phosphocholine ($T_m = 12$ °C). The images were obtained with the contact mode (set point ~ 600 pN).

After the strong rinse, the optical image showed a homogenous surface (Figure S3A) as it is also shown in the main text (Figure 2). The corresponding AFM image suggests a smooth surface with root mean square roughness (RMS) of 0.5 nm (RMS was taken within the while square in Figure S3C). The thickness of the SLB was studied by the scratch method,[1] commonly used in the determination of the surface-adsorbed polymer thickness. The cross section of the scratched area in Figure S3D suggests that the thickness of the SLB is 3 ± 1 nm, indicating that the SLB remained after the strong rinse is a single bilayer. Occasionally, nano-sized patches with a height of 4 nm were observed on the smooth surface (see the cross section of Figure S3C). They are the bilayer patches that remained even after the strong rinse.

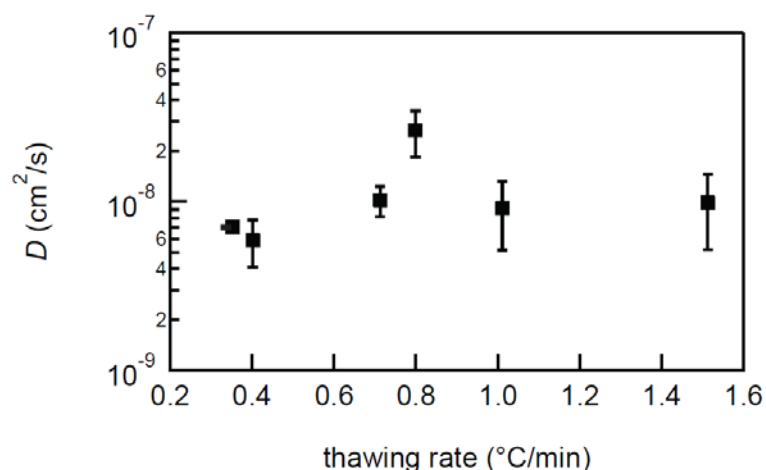**The freeze-thaw SLB assembly is insensitive to the thawing rate**

Figure S4 *Thawing rate dependence of the diffusion coefficient with POPC + TiO$_2$*

We investigated the thawing rate dependence on the SLB formation with POPC on TiO$_2$. Since the recovery fraction reached always more than 90 %, we estimated diffusion coefficient D for each sample, and plot it as a function of the thawing rate (Figure S4). Considering the error bars, no significant thawing rate dependence was detected in D,

implying that the SLB formation by freeze and thaw is insensitive to the thawing rate in this range.

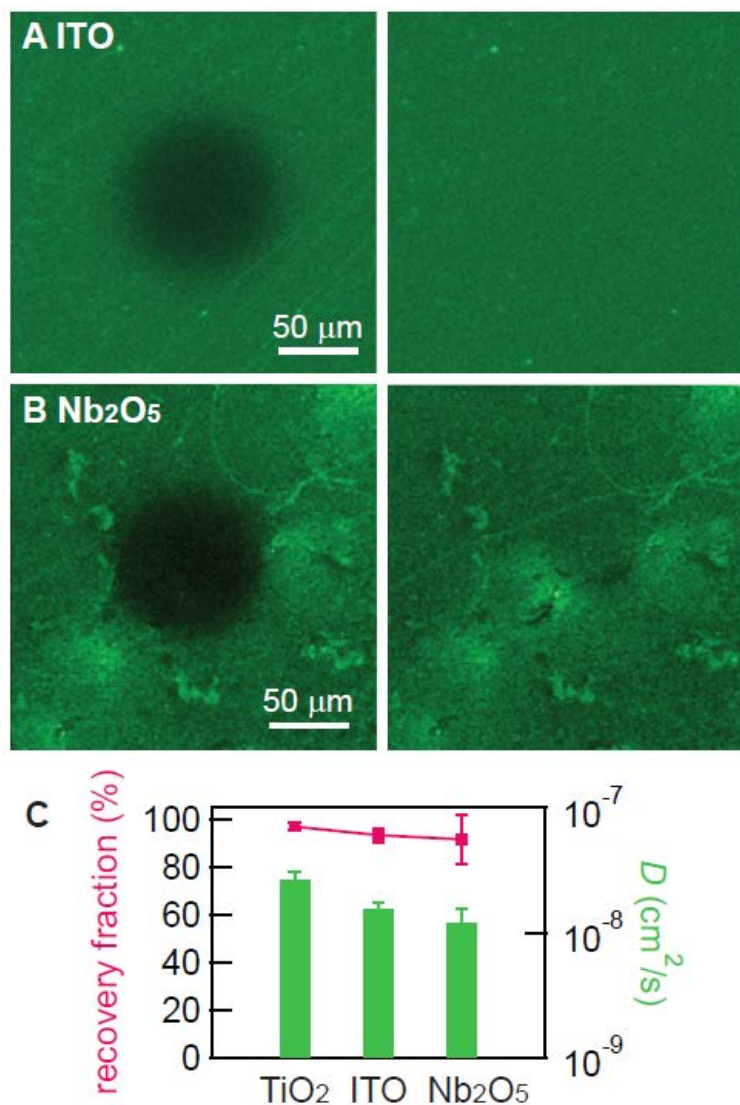## SLB formation by freeze and thaw on other substrates

Figure S5 *SLB formation by freeze and thaw on other substrates*

FRAP images right after photobleaching and 1 h later for **(A)** ITO and **(B)** Nb_2O_5 substrates. **(C)** Comparison of the diffusion coefficient and the recovery fraction between the different substrates.

To study the versatility of the freeze-thaw procedure, SLB formation with DOPC vesicles was investigated on different substrates. Transparent substrates were selected for the feasibility to obtain FRAP data with our inverted-microscope setup. FRAP images of the lipid

structures assembled on ITO (Figure S5A) and Nb_2O_5 (Figure S5B) are shown. ITO is a unique material that has both the optical transparency and the electric conductivity, frequently used in bioengineering. The fabrication of SLBs on ITO facilitates the simultaneous optical and electrical studies of lipids and membrane proteins.[2-3] Nb_2O_5 is another metal oxide used as a top layer surface or as an insulator for biosensors because of its biocompatibility.[4-5] Both for ITO and Nb_2O_5, DOPC vesicles adsorb intact as proved by the absence of recovery in FRAP experiments. After the freeze-thaw cycle, however, the bleached circle recovered for both surfaces (Figure S5AB). Note that the lipid patches and dots mentioned previously were removed by the strong rinse for these samples, resulting in relatively smooth surfaces. The comparison of D and the recovery fraction between TiO_2, ITO and Nb_2O_5 is shown in Figure S5C. It shows more than 90 % recovery on average, and D is in the same order as that of SLBs assembled by vesicle fusion on glass (3.9×10^{-8} cm^2/s) for all three substrates.[6] Considering the error bars, no clear substrate dependence was observed. POPC bilayers deposited on single crystalline TiO_2 and $SrTiO_3$ by Langmuir-Blodgett technique have both showed $D \sim 2 \times 10^{-8}$ cm^2/s without a significant substrate dependence similarly to our case, while the recovery fraction ($\sim$ 85 %) was lower presumably due to the unavoidable defects in the SLBs introduced by the fabrication method.[7] Langmuir-Blodgett technique is a versatile approach, which enables the fabrication of SLBs on many surfaces, although its low throughput and the inherit defects in the bilayers are the limitations. On contrary, the vesicle fusion forms defect-free SLBs in a self-assembling manner, however, it is not applicable for Nb_2O_5, and for TiO_2 without divalent ions. The result shows that the freeze-thaw technique has all the advantages of the self-assembly, versatility, and the quality of the formed SLBs comparable to the one by vesicle fusion.
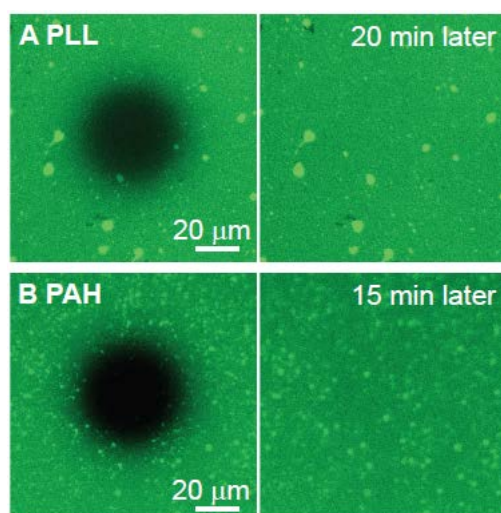
SLB formation on polycations by freeze and thaw

Figure S6 *SLB formation with POPC vesicles on polycations (poly-allylamine, PAH, Poly-L-lysine, PLL)*

Figure S6 shows the FRAP images of SLBs on polycations (poly-allylamine, PAH, Poly-L-lysine, PLL) that we fabricated by freeze and thaw. Polycations adhere on any type of plasma-treated surfaces, thus the data confirms that SLB-polycation composites can be deposited on any substrates. It further proves the versatility of the method.

1. K. Sugihara, J. n. Vörös and T. Zambelli, *The Journal of Physical Chemistry B*, 2010, null-null.
2. H. Hillebrandt and M. Tanaka, *The Journal of Physical Chemistry B*, 2001, **105**, 4270-4276.
3. K. Sugihara, M. Delai, I. Szendro, O. Guillaume-Genti, J. Vörös and T. Zambelli, *Sensors and Actuators B: Chemical*.
4. S. Pasche, S. M. De Paul, J. Voros, N. D. Spencer and M. Textor, *Langmuir*, 2003, **19**, 9216-9225.
5. N. P. Huang, J. Voros, S. M. De Paul, M. Textor and N. D. Spencer, *Langmuir*, 2002, **18**, 220-230.
6. D. M. Soumpasis, *Biophys. J.*, 1983, **41**, 95-97.
7. B. A. Nellis, J. H. Satcher Jr and S. H. Risbud, *Acta Biomaterialia*, 2011, **7**, 380-386.